Journal of Alloys and Compounds 509 (2011) 551–555

Contents lists available at ScienceDirect

Journal of Alloys and Compounds

journal homepage: www.elsevier.com/locate/jallcom

Electrochemical syntheses of soft and hard magnetic $Fe_{50}Pd_{50}$-based nanotubes and their magnetic characterization

Kristina Žužek Rožman*, Darja Pečko, Larisa Suhodolčan, Paul J. McGuiness, Spomenka Kobe

Jožef Stefan Institute, Jamova 39, Ljubljana, Slovenia

ARTICLE INFO

Article history:
Received 9 August 2010
Received in revised form
15 September 2010
Accepted 17 September 2010
Available online 25 September 2010

Key words:
Intermetallics
Nanostructured materials
Magnetization
Phase transitions
Magnetic measurements

ABSTRACT

Near-equiatomic Fe–Pd-based nanotubes with diameters of 200 nm and lengths of 1 μm were directly electrodeposited from a single electrolyte into polycarbonate templates. The as-deposited $Fe_{50}Pd_{50}$ nanotubes were then characterized compositionally, structurally and magnetically. The as-deposited $Fe_{50}Pd_{50}$ tubes had an *fcc* crystal structure and were magnetically soft ($H_C \approx 10$ kA/m), with the easy axis of the magnetization being parallel to the axes of the tubes. Angular-dependence measurements of the coercivity, where the hysteresis loops were measured as a function of the angle (θ) of the applied demagnetizing field, revealed a combination of magnetization reversal mechanisms, consisting of the curling mechanism, which dominates at low angles, with a transition to coherent rotation at angles $\geq 70°$. The development of the coercivity with annealing temperature due to the $L1_0$ ordering was also investigated. For this purpose the as-deposited nanotubes were annealed at temperatures from 400 °C to 650 °C for 1 h in Ar + 7% H_2 and the phase formation, the microstructure and the magnetic properties were analyzed. A maximum in the coercivity of 135 kA/m was achieved upon annealing at 550 °C.

1. Introduction

$Fe_{50}Pd_{50}$-based materials with an ordered *fct* structure, also referred to as the $L1_0$ structure, are of great importance because of their large magnetocrystalline anisotropy field (280 kA/m) along the *c*-axis direction of the tetragonal crystal structure, which makes them promising materials for high-density perpendicular magnetic recording media. In comparison with $L1_0$ Fe–Pt (915 kA/m) and Co–Pt (995 kA/m) the magnetocrystalline anisotropy of Fe–Pd is relatively modest, but since its ordering temperature is much lower than that of Fe–Pt and Co–Pt, Fe–Pd could be a suitable material for nanostructured magnetic recording media.

Fe–Pd nanostructures in the form of thin films were already prepared via physical vapor deposition methods—see, for example, Ref. [1]. On the other hand, there are only a few reports on the electrodeposition of Fe–Pd; this is due to the difficulty in preparing a stable electrolyte. Because of the large difference of 1.4 V [2] in the standard reduction potentials of Fe^{2+} and Pd^{2+}, different complexing agents have to be used in order to make the co-deposition of both metals possible. As a result, Fe–Pd thin films were successfully deposited from ammonium tartrate- [3], sulfate- [4] and citrate-based [5,6] baths.

In this study we used an electrolyte based on ammonium citrate, proposed in Ref. [5], which we used successfully in our previous study on equiatomic Fe–Pd thin films [7]. However, the main challenge we faced here was that the complexity of the deposition process increases when the aim is to deposit nanostructures into a porous template; this is because of the slow diffusion due to the deposition into long template channels and the low conductivity surface. So far, Liu et al. [8] have reported on the deposition of Fe–Pd nanotubes into alumina templates from a complex bath that consisted of ammonium citrate, citric acid and ammonium chloride and recently Haehnel et al. [9] reported on the Fe–Pd nanowire synthesis into alumina templates from complexed ammonium-sulfosalicylic electrolyte. Here we report on the successful deposition of Fe–Pd nanotubes from a simple plating bath based only on ammonium citrate. We have focused our study on compositions around $Fe_{50}Pd_{50}$ and investigated the structural and magnetic properties, with the emphasis on the $L1_0$ phase evolution and its effect on the coercivity.

Since coercivity is an important ferromagnetic property for many applications, an understanding of the magnetization reversal mechanism is very important. In bulk ferromagnetic materials the energy of the system is minimized by forming multiple magnetic domains. However, when the particle size becomes very small, only

* Corresponding author at: Jozef Stefan Institute, Jamova Cesta 39, 1000 Ljubljana, Slovenia. Tel.: +386 1 4773 877; fax: +386 1 4773 221.
E-mail address: tina.zuzek@ijs.si (K.Ž. Rožman).

0925-8388/$ – see front matter © 2010 Elsevier B.V. All rights reserved.
doi:10.1016/j.jallcom.2010.09.108

a single domain can exist within an individual particle, with the critical size of a single-domain particle being estimated [10] as follows:

$$r_{sd} = \left[\frac{6A}{N_c {M_S}^2}\left(\ln\left(\frac{2r_{sd}}{a_1} - 1\right)\right)\right]^{1/2} \quad (1)$$

where A is the exchange stiffness, M_S is the saturation magnetization, a_1 is the near-neighbor spacing and N_c is the demagnetizing factor. For a single-domain particle the two most common magnetization reversal modes can be modeled by coherent rotation or curling. However, for one-dimensional magnetic structures the mechanism was found to also depend on the outer diameter of the nanocylinders, where for a specific material the critical diameter d_c for the transition from uniform (coherent) rotation to curling can be calculated [11].

$$d_c = 2.08\left(\frac{A^{1/2}}{M_S}\right) \quad (2)$$

These two mechanisms lead to different values for the coercivity (H_C) and for the squareness (SQ), which can be calculated as M_R/M_S, depending on the direction/angle (Θ) of the applied field with respect to the axis of the tube [10]. Whereas the shapes of the H_C (Θ) curves are determined by the magnetization reversal mechanism, the SQ(Θ) curves, on the other hand, change as the overall easy axis of the tubes changes. Magnetization switching in ferromagnetic nanotubes was found to consist of both: the curling mechanism, which dominates at low angles, and coherent rotation, which dominates at high angles and was found to be dependent on the tube-wall thickness [12,13]. These findings are also in agreement with theoretical studies, which have shown that a decrease in the tube-wall thickness and of the external radii of the tubes enhances the stability region of the curling reversal mode, i.e., increases the transition angle between the curling and the coherent rotation [14]. In our study, angular-dependence measurements were performed in order to determine the particular magnetization reversal mechanism in the as-deposited *fcc* Fe–Pd nanotubes. The obtained results were then compared with the theoretical studies.

2. Experimental

The Fe–Pd-based nanotubes were electrochemically deposited from an electrolyte based on 14-mM $FeCl_2$, 6-mM $PdCl_2$ and 0.2-M $(NH_4)_2C_6H_6O_7$. Glass covered with 30 nm of Cr and 100 nm of Au (SiO_2/Cr/Au) was used as the template holder. The template used in this study was a track-etched polycarbonate (PC) membrane. The bottom of the PC membrane, with an average pore diameter of 200 nm and a thickness of 10 μm, was sputtered with Au for 300 s. This PC template was then glued from all sides (in order to promote the deposition from the top only) onto the SiO_2/Cr/Au substrate and used as a cathode. Potentials of −1.3 V down to −1.8 V, referenced against a Ag/AgCl electrode, and times of 900 s were used for the potentiostatic depositions. The pH was adjusted to 9 using NH_4OH. All the depositions were performed at room temperature, during which time the solution was constantly stirred using a magnetic stirrer. For the purposes of the microstructural, chemical and crystal structure analyses the as-deposited Fe–Pd-based nanotubes were released from the PC template by dissolving it in an organic solvent, dichloromethane (CH_2Cl_2). The as-deposited nanotubes were annealed in Ar + 7% H_2 (forming gas) from 400 °C up to 650 °C for 1 h. The Fe–Pd-based nanotubes were characterized using a field-emission-gun scanning electron microscope (FEG-SEM) JEOL JSM-7600F equipped with an energy-dispersive X-ray spectroscopy (EDXS) system INCA Oxford Instruments. A quantitative, standardless EDXS method with a virtual standards data library, combined with a spectral acquisition time of 60 s and a beam energy of 10 keV, was used to analyze the composition of the Fe–Pd-based nanotubes. The crystal structure of the as-deposited and annealed Fe–Pd-based nanotubes was investigated by X-ray diffraction (XRD) using a diffractometer (D4 Endeavor, Bruker AXS, Karlsruhe, Germany) with Bragg–Brentano geometry, a Cu Kα radiation source and a Sol-X energy-dispersive detector. The magnetic measurements were performed using a Lakeshore vibrating-sample magnetometer (VSM).

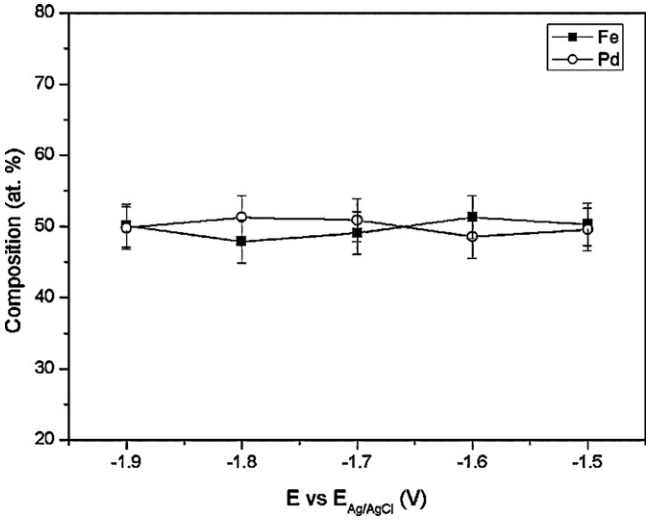

Fig. 1. Dependence of the composition of the Fe–Pd nanostructures on the applied voltage.

3. Results and discussion

Fig. 1 shows the dependence of the Fe/Pd ratio on the applied voltage for the deposited, one-dimensional nanostructures. From this it is clear that a near-equiatomic ratio between the Fe and Pd, determined with the EDXS, is achieved at an applied voltage of −1.5 V. Changing the applied voltage does not affect the composition of the deposited nanostructures, which is typical for processes where the mass transport is the slowest reaction and governs the whole deposition process. Slow diffusion is also one of the necessary conditions for the direct formation of tubes, which can be attributed to the relative rates of the kinetics and the diffusion of the Fe^{2+} and Pd^{2+} electropositive species into the templates [15,16]. Fig. 2 shows an array of $Fe_{50.3\pm3}Pd_{49.7\pm3}$ nanotubes deposited at −1.5 V for 900 s after the removal of the template. The tubes are uniform in their diameter (200 nm), which is determined by the template. The length of the as-deposited nanotubes is ∼1 μm, with some inconsistencies. A possible reason for that lies in the severe conditions associated with the dissolution of the PC template, which involved several centrifugation steps. A higher magnification micrograph in the top-left-hand corner of Fig. 2 shows that the

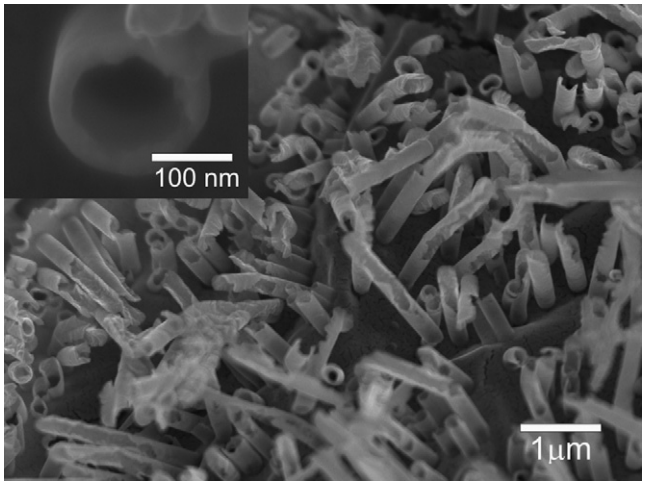

Fig. 2. FEG-SEM micrograph of the Fe–Pd-based nanotubes potentiostatically deposited for 900 s at −1.5 V after removal of the PC template. A higher magnification micrograph of a single nanotube is shown in top left corner.

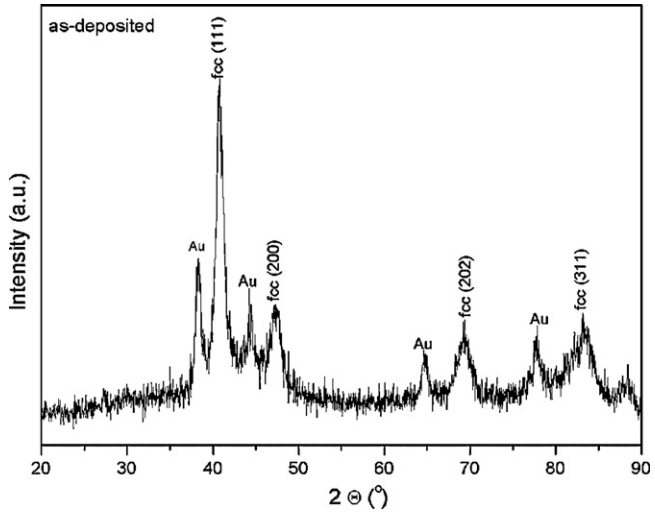

Fig. 3. XRD pattern of the as-deposited $Fe_{50}Pd_{50}$ nanotubes deposited at −1.5 V for 900 s.

diameter of a single nanotube, which was measured to be 210 nm, is very close to the pore diameters in the PC template (200 nm), and that the tube-wall thickness is around 40 nm. Fig. 3 shows the X-ray diffractogram of the as-deposited $Fe_{50}Pd_{50}$-based nanotubes deposited at −1.5 V for 900 s; this consists of the *fcc* Fe–Pd phase reflections together with the reflections coming from the Au conductive layer, which was sputtered on the back of the PC template.

Fig. 4 shows the hysteresis loop of the nanotubes inside the PC template deposited at −1.5 V for 900 s. The magnetic response was measured with the magnetic field parallel and perpendicular to the axes of the tubes. The as-deposited sample measured in the parallel geometry exhibits soft magnetic behavior with a modest coercivity of 9 kA/m, which is in accordance with the XRD results that showed that the as-deposited nanotubes consist of the *fcc* crystal structure, which has a low magnetocrystalline anisotropy [17]. The easy axis of the magnetization was found to lie parallel to the axes of the tubes. A slightly higher coercivity (11 kA/m) and lower squareness was observed in the perpendicular direction. The direction of the easy axis is in agreement with this direction being preferred in one-dimensional nanostructures, but it was found to depend on the dimensions of the one-dimensional nanostructures. In order to investigate the magnetic behavior of the array of nanotubes,

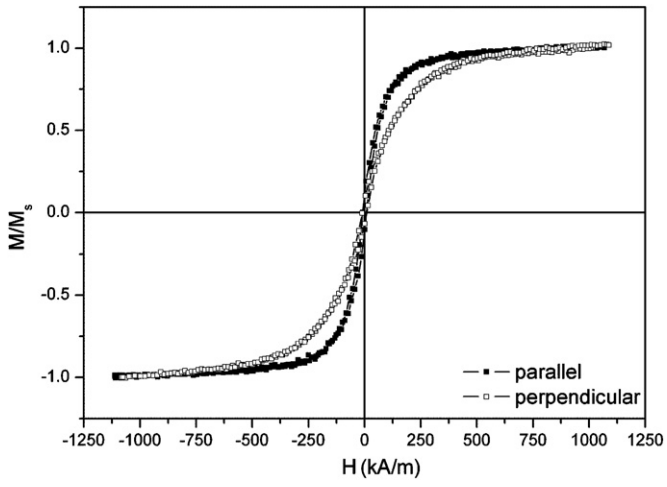

Fig. 4. Magnetic hysteresis loop for $Fe_{50}Pd_{50}$ nanotubes deposited at −1.5 V for 900 s inside the PC template measured in the parallel and perpendicular directions.

an interaction model proposed by Han et al. [18] was used. For reasons of simplicity the tubes were treated as nanowires. They discussed that the crossover of the easy axis from the parallel to the perpendicular direction happens if the effective anisotropy field is negative. According to the interaction model the total effective anisotropy field H_k can be calculated as follows:

$$H_k = 2\pi M_S - \frac{6.3 M_S d^2 L}{D^3} + H_{ma} \quad (3)$$

where $2\pi M_S$ is the contribution of the shape anisotropy, which is reduced by the magnetostatic interactions (the second term in Eq. (3)) that depend on the nanotube diameter d, the length of the tubes L, and the intertube distance D. Therefore, in densely packed nanowires the magnetostatic dipole or multipole interaction can reduce the total effective anisotropy and the coercivity in comparison with the isolated nanowire. However, this provides a simplified approach to determining the magnetostatic interaction. Escrig et al. [19] calculated the interaction energy between two identical nanotubes, where the interaction energy was found to decrease with an increasing interwire distance and a decreasing tube-wall thickness. Since the magnetocrystalline anisotropy (H_{ma}) of *fcc* Fe–Pd is very low, the last term in the equation is negligible, and therefore the effective anisotropy originates from the shape anisotropy, which is reduced by the magnetostatic interactions between the tubes. For our particular case, where $r = 200$ nm, $L = 1000$ nm and $D \sim 500$ nm, because the pore distribution is not regular in the PC template and the pores are far apart [16], the overall anisotropy field can be expressed as:

$$H_k = M_S(2\pi - 0.32) \quad (4)$$

The shape anisotropy is equal to $2\pi M_S \approx 6.4$ kA/m, which is three orders of magnitude larger than the magnetostatic interactions ($0.32\ M_S \approx 3.2$ A/m); this results in a positive effective anisotropy and therefore in an easy axis of magnetization in the parallel direction.

The angular dependences of the coercivity and the squareness were measured in order to investigate the mechanism of magnetization reversal. First, the critical radius (r_{sd}) for single-domain behavior for the as-deposited $Fe_{50}Pd_{50}$ was calculated from Eq. (1), using the parameters $A = 1.8 \times 10^{-6}$ erg/cm, $M_S = 1040$ emu/cc [20], $a_1 = 0.3852$ nm and $N_c = 0.04$. The critical radius equals ≈170 nm (diameter—$d = 340$ nm), which would imply that the Fe–Pd nanotubes act as single-domain particles. Furthermore, the critical diameter (d_c) for the transition from coherent to non-coherent rotation was calculated from Eq. (2) and is $d_c \approx 30$ nm, which means that the diameter of the Fe–Pd nanotubes (200 nm) is much larger than the critical value for coherent rotation. Therefore, the magnetization reversal is expected to proceed via the curling mechanism. However, since it is known that the thickness of the nanotube wall influences the reversal mechanism in magnetic nanotubes, we have investigated the magnetization reversal behavior in Fe–Pd nanotubes by applying angular-dependence measurements. The hysteresis loops of the as-deposited Fe–Pd-based nanotubes were measured with the external field applied at different angles (Θ) to the tubes axes. When the external magnetic field was parallel to the tubes' axes, then $\Theta = 0^\circ$, and when the field was applied perpendicular to the tubes' axes, then $\Theta = 90^\circ$. The dependences of the coercivity and the squareness (M_R/M_S) of the as-deposited nanotubes on the direction of the applied external field are presented in Fig. 5. A bell-shaped M_R/M_S curve was observed, which is in accordance with the easy axis of the magnetization being parallel to the tubes' axes. For the coercivity a counter-bell-shaped behavior is observed when increasing the angle up to $\Theta < \pm 70^\circ$, which suggests that the magnetization reversal proceeds via the curling mechanism. However, when increasing the angle above 70° a decrease in the coercivity is observed, implying a transition of the

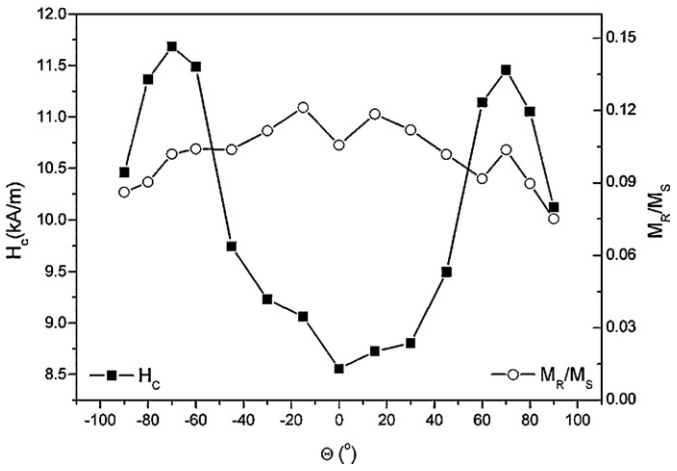

Fig. 5. Angular dependence of the coercivity and squareness of the $Fe_{50}Pd_{50}$ nanotubes deposited at −1.5 V for 900 s inside the PC template.

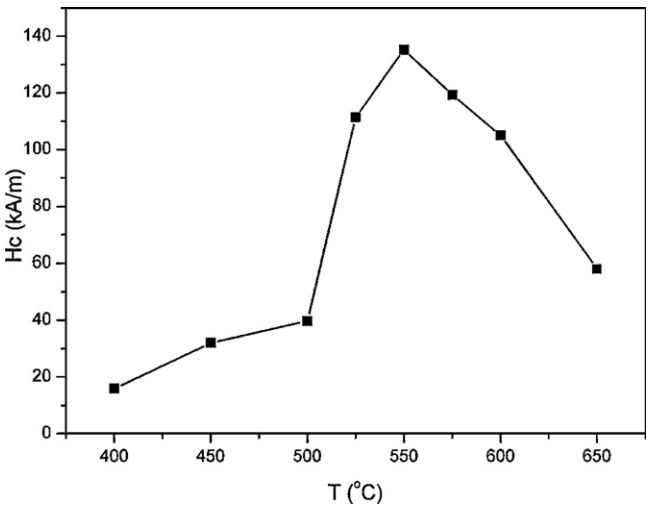

Fig. 6. Dependence of the coercivity of the $Fe_{50}Pd_{50}$ nanotubes on the annealing temperature (all the samples were annealed for 1 h in forming gas).

magnetization behavior from the curling- to the coherent-type mechanism, suggesting that when the applied field angle is small then the magnetic moments align preferentially parallel to the tube axis and the magnetization reversal takes place via the curling mechanism, and when the field angles are large the moments align perpendicular to the tube axis and a coherent reversal mode is observed. This kind of mixed behavior was already reported and explained for different ferromagnetic nanotubes [12,13]. The transition angle where the magnetization mechanism changes from curling to coherent, calculated by Escrig et al. [14], was found to depend on the thickness of the nanotube wall and the external diameter of the tubes. They showed that increasing the ratio between the external and the internal diameter of the nanotubes, which means decreasing the wall thickness, results in an increase in the transition angle between the curling and the coherent rotation mechanisms. Furthermore, the calculation showed that the transition angle is increased by increasing the external radius of the tubes. Similar behavior was also observed by Sharif et al. [13], where they showed that the tube-wall thickness indeed influences the magnetization reversal behavior in ferromagnetic nanotubes. By increasing the tube-wall thickness the prevailing mechanism became curling, if the external diameter of the nanotubes was large. However, a thinner wall thickness resulted in a combined type of magnetization reversal behavior where at larger angles the coherent rotation was dominant, while at low angles curling was the prevailing mechanism. For Fe–Pd nanotubes the coercivity was found to increase with an increasing angle θ from 0° to 70°, which is in good agreement with the curling model; however, above this critical angle the coercivity decreases abruptly. It can therefore be concluded that at large angles coherent rotation is dominant, while curling occurs at angles $\theta \leq 70°$. As already explained by Han et al. [12], the distinct geometry of the nanotubes represents two configurations of the magnetic moments. When the applied field angle is small, then the moments will align parallel to the tube axis and the magnetization reversal will proceed via curling rotation. On the other hand, at large field angles, the moments will align perpendicular and the reversal will take place as a coherent rotation. Different alignments of the magnetic moments are attained in the magnetic nanotubes because of the influence of the wall thickness, which causes the transition from curling to coherent at higher angles.

In order to increase the coercivity of the as-deposited Fe–Pd-based nanotubes, a series of annealing experiments was performed. After the deposition the as-deposited nanotubes were annealed at temperatures between 400 °C and 650 °C in forming gas for 1 h. The magnetic properties measured after the annealing process correspond to a sample that consisted of randomly orientated nanotubes, as a result of the polymeric nature of the template that burned off during the thermal treatment. Fig. 6 shows the development of the coercivity upon annealing. The highest coercivity of 135 kA/m was achieved after annealing at 550 °C for 1 h; this exceeds the values obtained for electrodeposited equiatomic Fe–Pd thin films [5,7], most probably because of the substrate-free system, which was found to react with the Fe–Pd alloy upon annealing [7]. Increasing the annealing temperature above 550 °C resulted in a decrease of the coercivity.

Fig. 7 shows the XRD patterns of the samples annealed at 550 °C and 650 °C. The high coercivity obtained after annealing at 550 °C can be attributed to the $L1_0$ ordering, the evidence for which is the appearance of the super-structural (1 1 0) reflection at $2\Theta = 32.8°$ and the (2 0 0) reflection splitting into the (2 2 0) and (0 0 2) reflections, which appear in addition to the *fcc* reflections observed in the XRD pattern of the as-deposited nanotubes (Fig. 3). While the coercivity was found to increase with temperature up to 550 °C, higher temperatures resulted in a coercivity decrease. Fig. 7 also shows the XRD pattern of the sample that was annealed at 650 °C for 1 h. Most of the reflections correspond to the Pd-rich $L1_2$ phase with the composition of $FePd_3$ and the remains of the $L1_0$ phase,

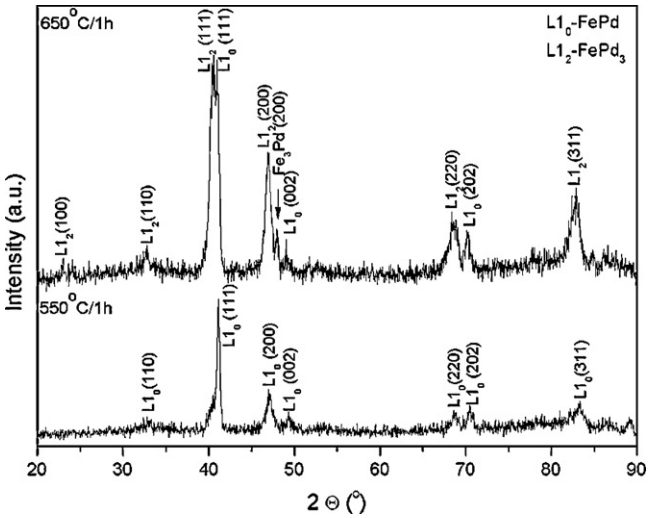

Fig. 7. The XRD patterns of the $Fe_{50}Pd_{50}$ nanotubes annealed at 550 °C and 650 °C for 1 h in forming gas.

together with a reflection at $2\Theta = 47.9^\circ$, which can be attributed to the Fe_3Pd phase. Based on these facts it can be concluded that the desired ordering into the $L1_0$ phase only happens in the temperature interval between 400 °C and 550 °C. A further increase in the annealing temperature results in the formation of the soft magnetic $FePd_3$ and Fe_3Pd phases, which were found to decrease the coercivity. This Fe_3Pd soft magnetic phase was already reported to decrease the coercivity in an equiatomic Fe–Pd nanoparticle system [21]. In addition, in annealed Fe–Pd nanotubes the shape anisotropy is not the predominant anisotropy because of the development of the $L1_0$ Fe–Pd phase, with its high magnetocrystalline anisotropy. The induced grain growth with increasing temperature of the phase having high magnetocrystalline anisotropy leads to a wide distribution of the direction of the net easy axis. This can lead to wide variations in the switching fields [22] and a coercivity decrease in annealed Fe–Pd nanotubes. However, although larger grains are likely to play some minor role in reducing the coercivity, almost certainly the overriding effect comes from the presence of the soft magnetic $FePd_3$ and Fe_3Pd phases.

Since the nanotube ordering was lost after the annealing treatment, the angular dependence measurements and of hard magnetic Fe–Pd nanotubes were not performed. In order to investigate the magnetization reversal mechanism in $L1_0$-based Fe–Pd nanotubes a thermally stable template like alumina will have to be used, which is the aim of our future investigations.

4. Conclusions

Equiatomic Fe–Pd-based nanotubes were directly deposited into PC templates using the electrochemical method. The as-deposited *fcc* $Fe_{50}Pd_{50}$ tubes were magnetically soft. The easy axis of the magnetization was found to be parallel to the axes of the tubes, which was also confirmed with the interaction model calculations. The angular-dependence measurements showed that the magnetization reversal mechanism in the as-deposited $Fe_{50}Pd_{50}$-based nanotubes proceeds via a combined mechanism, where the curling is dominant at low angles ($\theta \leq 70^\circ$) and the coherent at high angles ($\theta \geq 70^\circ$). The coercivity of the as-deposited $Fe_{50}Pd_{50}$-based nanotubes was significantly increased by thermally induced $L1_0$ ordering, which was confirmed with XRD. The highest coercivity (135 kA/m) was achieved after annealing at 550 °C for 1 h in forming gas. Because of this low ordering temperature, in comparison with Co–Pt or Fe–Pt, Fe–Pd, this material could be suitable for nanostructured magnetic recording media.

Acknowledgements

This work was supported by Slovenian Research Agency (ARRS) via P2-0084-0106/05. The authors would also like to acknowledge Prof. X.F. Han from State Key Laboratory of Magnetism, Institute of Physics, Beijing, China, for his readiness for help in the scientific discussion.

References

[1] S. Inoue, K. Inoue, S. Fujita, K. Koterazawa, Mater. Trans. 44 (2003) 298–304.
[2] M.E. Brumgärtner, D.R. Gabe, Trans. Inst. Met. Finish. 78 (2) (2000) 79–85.
[3] S. Doi, F. Wang, K. Hosori, T. Watanabe, Mater. Trans. JIM 44 (2003) 649–652.
[4] K.J. Bryden, J.Y. Ying, J. Electrochem. Soc. 145 (1998) 3339–3346.
[5] S.C. Hernandes, B.Y. Yoo, E. Stefanescu, S. Khizroev, N.V. Myung, Electrochim. Acta 53 (2008) 5621–5627.
[6] F. Wang, S. Doi, K. Hosori, H. Yoshida, T. Kuzushima, M. Sasadaira, T. Watanabe, Electrochim. Acta 51 (2006) 4250–4254.
[7] D. Pečko, K. Žužek Rožman, P.J. McGuiness, B. Pihlar, S. Kobe, J. Appl. Phys. 107 (2010) 09A712.
[8] H. Liu, F. Wang, Y. Zhao, J. Liu, K.C. Park, M. Endo, J. Electroanal. Chem. 633 (2009) 15–18.
[9] V. Haehnel, S. Fähler, L. Schultz, H. Schlörb, Electrochem. Commun. 12 (8) (2010) 1116–1119.
[10] L. Sun, Y. Hao, C.-L. Chien, P.C. Searson, IBM J. Res. Dev. 49 (2005) 79–102.
[11] H. Zheng, R. Skomski, L. Menon, Y. Liu, S. Bandyopadhyay, D.J. Sellmyer, Phys. Rev. B 65 (2002) 134426.
[12] X.-F. Han, S. Shamalia, R. Sharif, J.-Y. Chen, H.-R. Liu, D.-P. Liu, Adv. Mater. 21 (2009) 4619–4624.
[13] R. Sharif, S. Shamalia, M. Ma, L.D. Lao, R.C. Yu, X.F. Han, M. Khaleeq-ur-Rahman, Appl. Phys. Lett. 92 (2008) 032505.
[14] J. Escrig, M. Daub, P. Landeros, K. Nielsch, D. Altbir, Nanotechnology 18 (2007) 445706.
[15] J. Fu, S. Cherevko, C-H. Chung, Electrochem. Commun. 10 (2008) 514–518.
[16] K. Žužek Rožman, S. Šturm, Z. Samardžija, P.J. McGuiness, S. Kobe, Mater. Chem. Phys. 118 (2009) 105–110.
[17] N. Miyata, K. Tomotsune, H. Nakada, M. Hagiwara, H. Kadomatsu, H. Fujiwara, J. Phys. Soc. Jpn. 55 (3) (1986) 946–952.
[18] G.C. Han, B.Y. Zong, P. Luo, Y.H. Wu, J. Appl. Phys. 93 (2003) 9202.
[19] J. Escrig, S. Allende, D. Albtir, M. Bahiana, Appl. Phys. Lett. 93 (2008) 023101.
[20] Y. Hirotsu, K. Sato, J. Ceram. Proc. Res. 6 (2005) 236–244.
[21] S. Kang, Z. Jia, D.E. Nikles, J.W. Harrell, J. Appl. Phys. 95 (11II) (2004) 6744–6746.
[22] R.M.H. New, R.F.W. Pease, R.L. White, IEEE Trans. Magn. 31 (6) (1995) 3805.